

## Low-Level Convergence Lines over Northeastern Australia. Part II: Southerly Disturbances

ROGER K. SMITH

*Meteorological Institute, University of Munich, Munich, Germany*

MICHAEL J. REEDER

*Centre for Dynamical Meteorology and Oceanography, Monash University, Clayton, Australia*

PETER MAY

*Bureau of Meteorology Research Centre, Melbourne, Australia*

HARALD RICHTER

*Bureau of Meteorology Training Centre, Melbourne, Australia*

(Manuscript received 11 July 2005, in final form 12 February 2006)

### ABSTRACT

Observations of northward-moving borelike convergence lines over the southern part of the Gulf of Carpentaria region of northern Australia are described. Eleven such disturbances were documented during the 45-day period of the 2002 Gulf Lines Experiment. Of these, six were classified as major and five as minor, depending on their coherence throughout the region. The mean synoptic conditions leading to the two types of events were found to differ. The data for the events provide further insight into the structure and origin of borelike disturbances in the region. Two of the major events, those of 28–29 September and 9 October, are particularly noteworthy. The first of these had a clear double-change structure at all surface stations in the southeastern gulf region with an undular borelike wave preceding and separating from an airmass change in the form of a dryline. It is probably one of the best documented cases of its type. The second, which was documented in unprecedented detail by an instrumented research aircraft, consisted of three separate disturbances: one moving from the southeast, one from the south, and one from the northeast, all of which collided over the gulf. It is believed that the aircraft measurements are the first of their kind anywhere in the world. The aircraft made two long low-level transects through the disturbances and a higher-level transect where they were colliding. Various soundings were also made. The aircraft data showed clearly the undular borelike nature of the southeasterly disturbance. Measured vertical velocities in the waves were as high as  $3 \text{ m s}^{-1}$  at a mean altitude of about 230 m. Vertical velocities as high as  $5 \text{ m s}^{-1}$  were measured in the region of the collision at an altitude of about 1 km. The longevity of the bores is not explained by the vertical structure of the Scorer parameter, which indicates a leaky waveguide.

### 1. Introduction

Part I of this two-part paper, Goler et al. (2006), documented the North Australian cloud lines (NACLs) observed in the Gulf of Carpentaria region of northeastern Australia during the Gulf Cloud Lines Experi-

ment (GLEXP), which was carried out in September and October 2002. In this second part, we document the low-level convergence lines, sometimes marked by cloud, that formed south of the gulf and moved northward. Such convergence lines were the subject of previous investigations by Smith et al. (1982, 1986), where they were referred to as “southerly nocturnal wind surges.” Those marked by cloud lines are referred to as “southerly morning glories.” Like their more frequent northeasterly counterparts in the region, southerly surges have been shown to have the character of an

---

*Corresponding author address:* Prof. Roger K. Smith, Meteorological Institute, University of Munich, Theresienstr. 37, 80333 Munich, Germany.  
E-mail: roger@meteo.physik.uni-muenchen.de

undular bore propagating on the nocturnal low-level stable layer (Smith et al. 1995). As discussed below, there is mounting evidence that such disturbances are a fundamental aspect of frontogenesis at low latitudes over the Australian continent.

Smith et al. (1986) showed that a feature of the synoptic mean sea level pressure patterns conducive to the formation of southerly surges over northern Australia is the extension of a ridge of high pressure across the continent directing a southerly to southeasterly airstream over western Queensland. In some cases, strong ridging occurs during the 12- to 24-h period prior to the surge and is preceded by the movement of a frontal trough across central Queensland; in other cases, the ridge is quasi stationary and the front (at least as commonly analyzed) is absent. However, the inland heat trough is always a prominent feature and forms along the leading edge of the ridge. It is well marked in model forecasts as a narrow line of enhanced low-level cyclonic vorticity and, from available observations, it appears to be coincident with the dryline.

It turns out that synoptic conditions favorable for southerly wind surges are often accompanied by a ridge of high pressure along the east coast of Australia, which is also conducive to the formation of the more common northeasterly surges discussed in Part I. Thus, both types of disturbances can occur on the same day. Smith et al. (1986) showed a rare ground-based cloud photograph of the interaction of two such disturbances (see their Fig. 4), but modern satellite imagery indicates that such events are relatively frequent. Spectacular examples of multiple surge interactions are detailed in Reeder et al. (1995) and in section 3 below.

Smith et al. (1986) discussed possible mechanisms for the genesis of southerly surges. These include

- the motion of a cold front into the developing low-level stable layer,
- the interaction between the nocturnal low-level jet and the deeply penetrating sea breeze from the southern gulf coast, and
- katabatic drainage from the Barkly Tablelands.

At the time of their investigations, little was known about the structure of cold fronts that move across central Australia into the Tropics and it was the desire to understand the nature and origin of southerly nocturnal wind surges in the southern gulf region that led to a series of field experiments to document the behavior of these fronts (Smith and Ridley 1990; Smith et al. 1995; Deslandes et al. 1999; Reeder et al. 2000; Preissler et al. 2002).

During the Central Australian Fronts Experiment (CAFE) in 1991, two fronts were documented in un-

precedented detail (Smith et al. 1995). The data obtained highlighted the large diurnal variation of the frontal structure associated with diabatic processes. The fronts are often difficult to locate during the late morning and afternoon when (dry) convective mixing is at its peak, but they develop strong surface signatures in the evening as the convection subsides and a surface-based radiation inversion develops. Moreover, there appears to be a ubiquitous tendency in the early morning for the formation of a nonlinear wavelike, or borelike,<sup>1</sup> structure at the leading edge of the frontal zone as the inversion strengthens. In each of the CAFE cases, as the bore developed, it was observed to propagate ahead of the airmass change on the preexisting inversion. In one case, the data provided the first clear evidence of the formation of a southerly morning glory bore disturbance in the Gulf of Carpentaria region from a cold front in the south. The observations were consistent with the idea that the penetration of a disturbance into the southern gulf region in the form of a southerly morning glory is favored by an evening passage of the front through Mount Isa. Then, the disturbance is not subject to the destructive effect of strong diabatic heating on its way to the gulf.

In this paper we present analyses of data collected on southerly wind surges obtained during GLEX. One event involving the multiple interaction of surges was documented in unprecedented detail, with measurements including data obtained during aircraft penetrations and aircraft soundings. Another event provides one of the best examples to date of the separation of a borelike disturbance from a cold front.

The paper is organized as follows: section 2 gives a summary of the southerly disturbances documented during GLEX and classifies these as either major or minor events. The two most interesting major events are examined at length in section 3, while another four are summarized briefly in section 4. The results are discussed in section 5, and conclusions are presented in section 6.

## 2. Southerly convergence lines

The instrument network for the experiment is detailed in Part I and the locations of places mentioned in

---

<sup>1</sup> Borelike means that there is an increase in the mean surface pressure with the diurnal variation removed following the passage of the disturbance. A pure bore is characterized by a sudden rise in pressure. In an undular bore, the pressure rise is accomplished by a series of large-amplitude waves. Unlike gravity currents, the relative flow in bores is from front to rear and any cooling behind the disturbance is associated with the lifting of air parcels rather than advection.

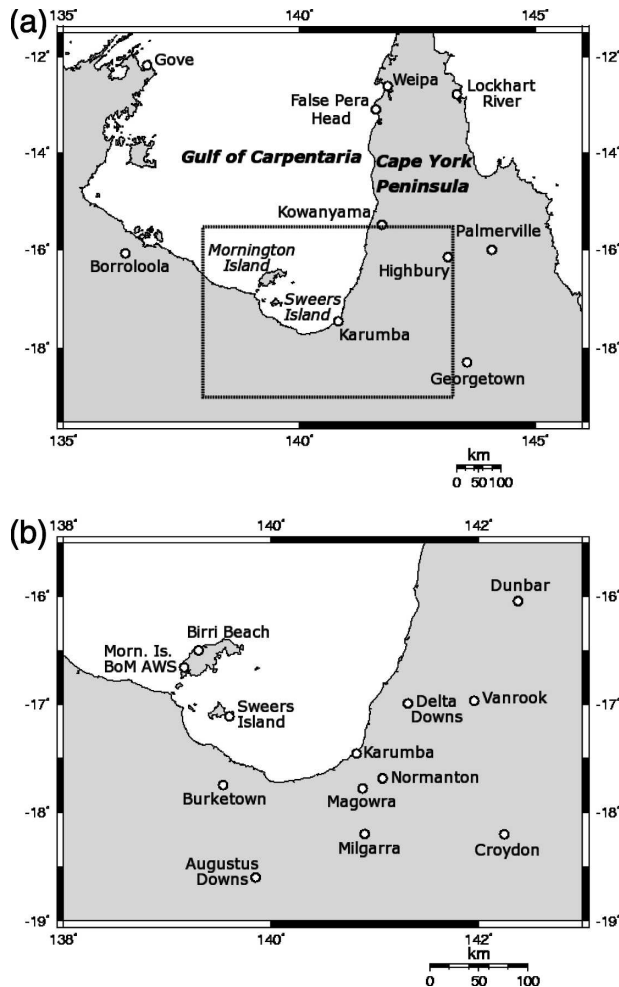


FIG. 1. Maps of (a) the Gulf of Carpentaria region and (b) a close-up of the southern gulf coastal region, marked by the rectangle in (a) showing the location of AWS stations. Other places mentioned in the text are marked.

the text are shown in Fig. 1. A total of 11 southerly disturbances were observed during the time period that two or more automatic weather stations (AWSs) were in operation (10 September until 22 October 2002). The time period for individual stations varied, but all stations were in operation during the period 19 September–17 October, except at Croydon where the data were intermittent. Table 1 lists the events together with their times of passage at Karumba or at some other station when not recorded at Karumba. These times are given in eastern standard time (EST).<sup>2</sup> An event is defined as a borelike disturbance identified by a sharp rise in surface pressure, possibly followed by a series of large-amplitude waves in which the mean pressure rises,

<sup>2</sup> EST = UTC + 10 h.

TABLE 1. List of southerly events documented during GLEX. Occurrence times for disturbances not detected at Karumba are given at selected stations.

Event	Date	Time (EST)	Major
1	10 Sep	0645 at Karumba	Yes
2	17 Sep	0820 at Karumba	Yes
3	23 Sep	0820 at Karumba	No
4	28 Sep	2355 at Karumba	Yes
5	4 Oct	0530 at Burketown	Yes
6	5 Oct	0305 at Karumba	No
7	6 Oct	0450 at Milgarra	No
8	9 Oct	0505 at Karumba	Yes
9	14 Oct	0330 at Milgarra	Yes
10	20 Oct	0445 at Milgarra	No
11	21 Oct	0145 at Milgarra	No

and detectable at a minimum of two stations. Typically the rise in pressure is accompanied by a sharp freshening of the wind and a marked change in wind direction. A major event is classified loosely as one for which the disturbance was detected at most or all of the southern AWS stations, while minor events were detected at only a few of the stations. Major and minor events are indicated in Table 1. All major events and some minor events were accompanied by a recognizable roll cloud or series of roll clouds observed from the ground or in satellite imagery. The interval between major events was approximately one week, while minor events sometimes occurred on successive days (events 6 and 11), or on days following major events (event 5). Two major events of particular significance were those of 28–29 September and 9 October 2002. The other four major events (events 1, 2, 5, and 9) are discussed briefly in section 4 and the minor events in section 5.

### 3. Two major events

#### a. Event 4: 28–29 September

A special feature of this event was the clear double-change structure at all AWS stations in the southeastern gulf region with an undular borelike wave preceding and separating from an airmass change in the form of a dryline. As in other major events (see section 4), it was accompanied by ridging over the northeastern part of the continent (Fig. 2), but in this case the ridging was strong enough to push the trough a considerable distance north over the gulf and the peninsula. As a result, there was a significant airmass change across much of the AWS network with dry continental air extending out over the gulf. At Karumba, there were strong southeasterly winds with blowing dust following the change.

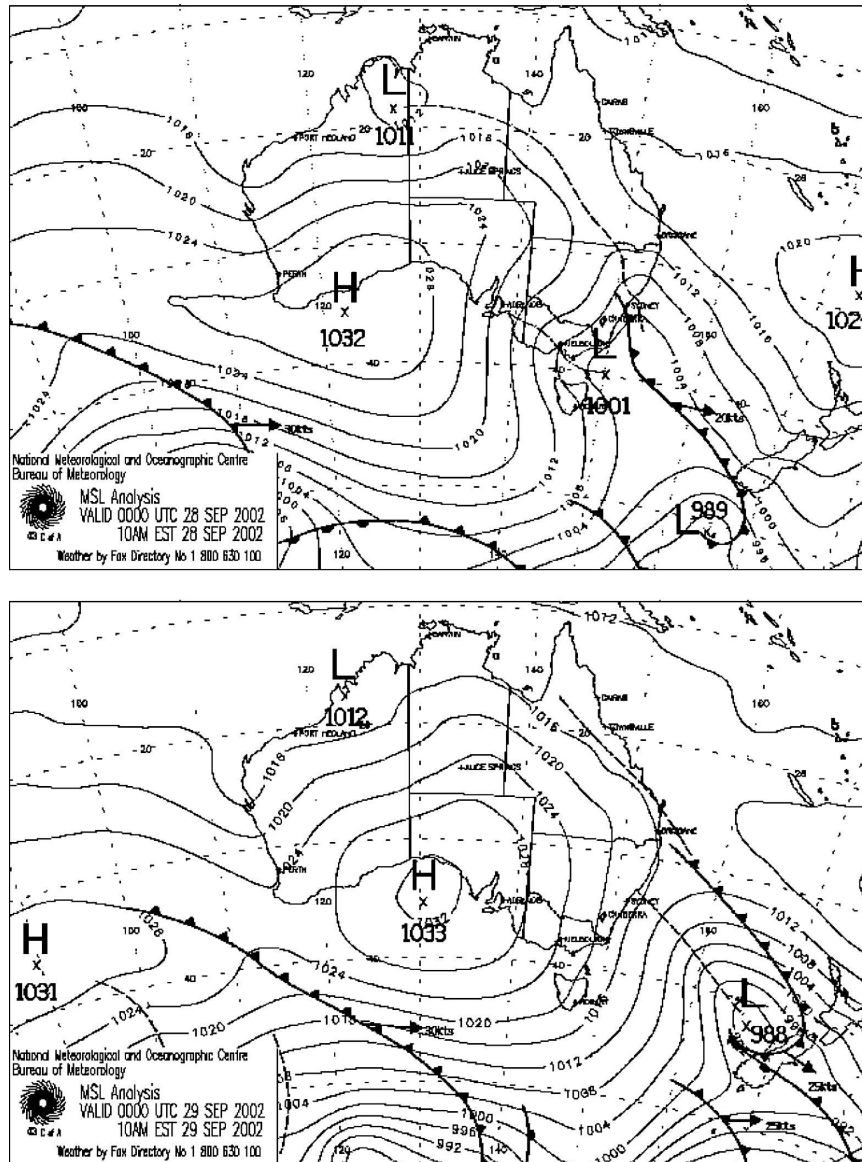


FIG. 2. Event 4: Bureau of Meteorology mean sea level pressure analyses at 1000 EST (top) 28 Sep and (bottom) 29 Sep 2002.

Figure 3 shows the time series of various quantities from two of the AWS stations: Augustus Downs (one of the southernmost stations) and Sweers Island in the gulf. At Augustus Downs, the bore wave is evident as a sharp pressure jump at about 2115 EST, accompanied by a sharp increase in wind speed and an abrupt change in wind direction from one slightly west of north to a southerly. A second wave of the bore with a further jump in pressure occurred about 15 min later. The passage of the dryline was marked by a sharp fall in the dewpoint at around 2300 EST, accompanied by a slight increase in temperature and a rapid freshening of the wind from the southeast.

The temperature increase with the disturbance passage seen at Augustus Downs is commonly observed at night over central and northern Australia with the passage of cold fronts and is a result of the downward mixing of potentially warm air across a strong but relatively shallow surface-based inversion (see, e.g., Smith et al. 1995, p. 23). Indeed, numerical model simulations of the present event indicate that the dryline does have the thermal characteristics of a shallow cold front in the lowest 2 or 3 km (Thomsen and Smith 2006). The surface data from Sweers Island show a similar structure, with the bore wave onset at about 0130 EST and the airmass change just before 0630 EST. Thus, the bore

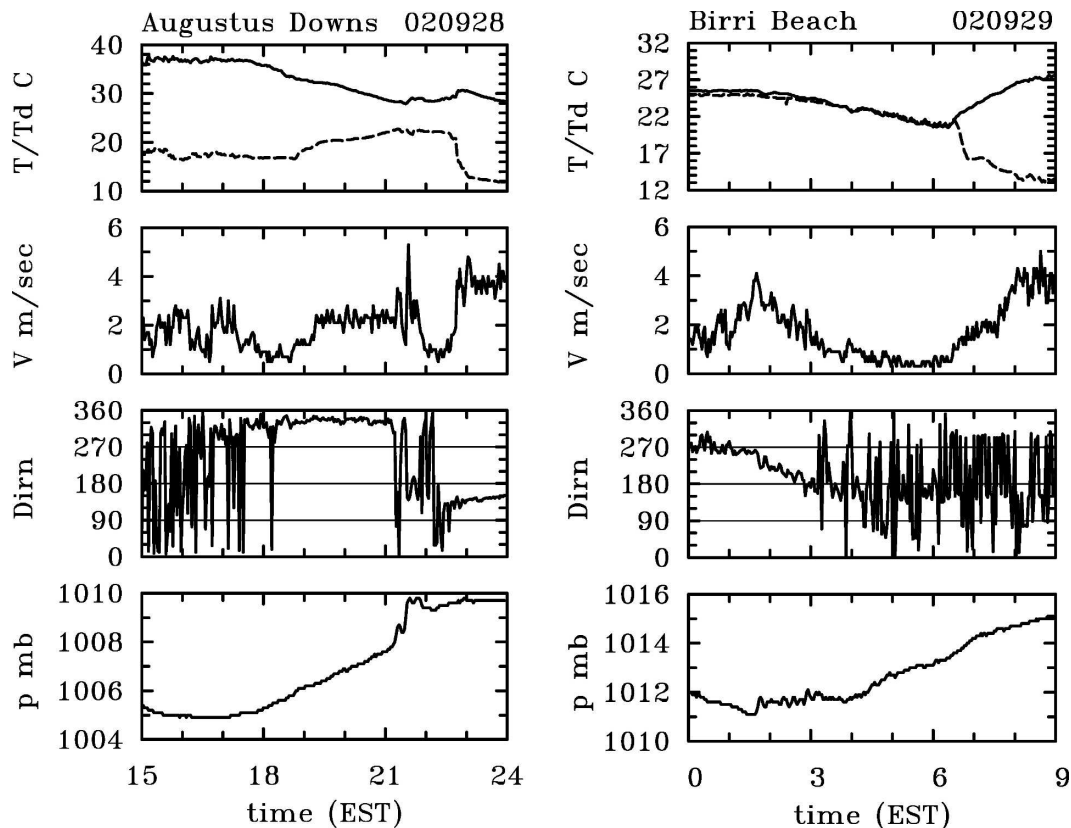


FIG. 3. Event 4: time series of temperature, dewpoint temperature (dashed), wind speed and direction, and pressure from the AWS stations at (left) Augustus Downs and (right) Birri Beach during the passage of the southerly disturbance of 28–29 Sep 2002.

wave had separated farther from the airmass change as the disturbance moved northward. This separation is seen clearly in Fig. 4, which shows the time series of surface pressure, temperature, and dewpoint at all AWS stations in the southeastern gulf region ordered by latitude.<sup>3</sup>

We do not know at what stage the disturbance developed cloud, but east–west oriented cloud lines in the first visible satellite image at 0630 EST (2200 UTC 28 September) indicated that by that time the bore wave had already reached the central part of the gulf.

There is mounting evidence that all borelike disturbances that originate from the south are associated with cold front–like disturbances that form overnight in the trough (Smith et al. 1982, 1986, 1995), but the present event is one of the best documented cases that we are aware of, comparable with the two cases documented during the Central Australian Fronts Experiment in

1991 (Smith et al. 1995). Figure 4 shows that there was not much of a temperature change recorded at the surface, although operational forecasts of the event using the mesoscale version of the Bureau of Meteorology's Limited Area Prediction System (meso-LAPS; Puri et al. 1998; see also Jackson et al. 2002) and corresponding simulations using the fifth-generation Pennsylvania State University–National Center for Atmospheric Research Mesoscale Model (MM5; Thomsen and Smith 2006) do indicate a relatively deep layer of cooler air following the change. This is not necessarily inconsistent with the surface observations, which as noted above, often show a *rise* in surface temperature accompanying the passage of a cold front over central Australia.

#### b. Event 8: 9 October

In this event, one of the most visually spectacular documented during GLEX, southerly, southeasterly, and northeasterly morning glories collided over the gulf near Mornington Island. There was a NAEL over the northern gulf also. The Cessna 404 instrumented re-

<sup>3</sup> UTC is used in this plot for ease of plotting, because it seeks to show relative times.

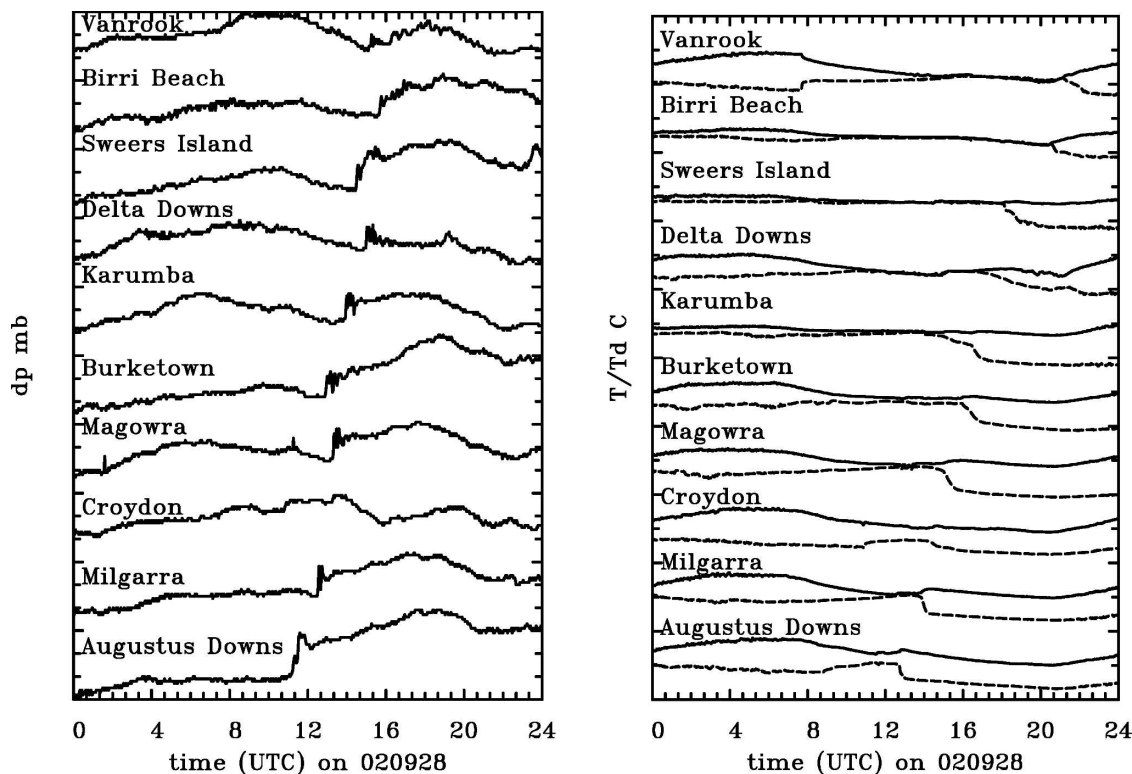


FIG. 4. Event 4: (left) Pressure traces with mean diurnal variation and diurnal trend removed and (right) temperature and dewpoint (dashed) traces at AWS stations in the southeastern gulf region on 28 Sep 2002. Times in this figure are UTC, which is 10 h behind EST. Stations are ordered by latitude.

search aircraft made measurements of the three disturbances over the southern part of the gulf including traverses through them, several vertical soundings, and measurements of the waves around the time of the collision.

The synoptic situation is shown in Fig. 5 and was similar to that in event 4. The mean sea level pressure pattern at 2200 EST 8 October (1200 UTC) comprised a weak low over the southeastern part of the continent, a trough that curved northwestward from the parent low to the gulf region, and a strong ridge across central Australia (top panel of Fig. 5). A ridge extended northwestward along the east coast of Australia also. Twelve hours later (bottom panel of Fig. 5) the anticyclone had expanded, and the trough, which marks the leading edge of the anticyclone, had pushed northward and eastward toward the gulf.

Sometime overnight, southerly, southeasterly, and northeasterly morning glory disturbances developed. The most prominent feature in the Geostationary Meteorological Satellite (GMS) visible image at 0832 EST 9 October is the series of cloud lines in the southeastern corner of the gulf (Fig. 6). The family of cloud lines

oriented northeast–southwest is the southeasterly morning glory. There is also a cloud line oriented northwest–southeast, marking the northeasterly morning glory, and a group of cloud lines essentially oriented east–west marking the southerly morning glory. The wave crests of each family are noticeably curved in the region in which they intersect. A weak NACL is also visible in the northeastern part of the gulf.

The southeasterly disturbance arrived at Karumba at 0505 EST, while the northeasterly arrived there at 0530 EST. Time series of temperature, dewpoint temperature, wind speed and direction, and pressure at Sweers Island and Augustus Downs are shown in Fig. 7. The southerly and southeasterly morning glories passed Sweers Island at 0645 EST and 0740 EST, respectively. The pressure perturbations were accompanied by fluctuations in wind speed and direction, with the maximum gusts of about  $8 \text{ m s}^{-1}$  recorded at a height of 2 m. The time at which the weaker northeasterly passed Sweers Island appears to be about 0850 EST, although there is a degree of uncertainty as the signal is superimposed on that from the trailing southerly and southeasterly waves.

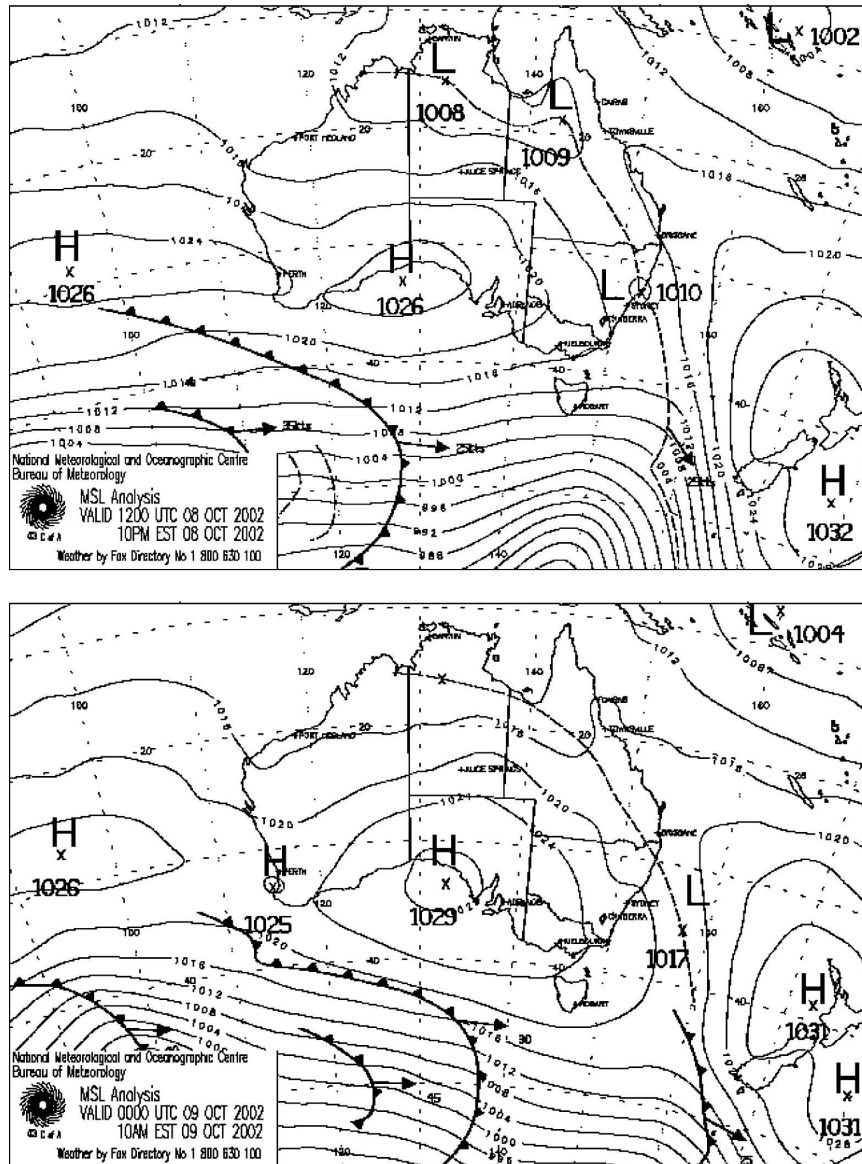


FIG. 5. Event 8: MSLP analyses at (top) 2200 EST 8 Oct and (bottom) 1000 EST 9 Oct 2002.

The AWS trace at Augustus Downs shows the passage of a single southerly disturbance at 0400 EST marked by a sharp rise in the pressure, a slight decrease in the temperature and dewpoint temperature, and an increase in the wind speed. Ahead of the disturbance the wind was southwesterly but, as the disturbance approached, the wind backed to become southerly. Our data are inadequate to determine whether this disturbance was the southerly or southeasterly disturbance. The trace also shows the passage of the trough and dryline, which arrive at 0715 EST and are marked by a pronounced decrease in dewpoint temperature, an

increase in wind speed, and the onset of a strong south-southeasterly flow.

### c. Radar observations

The southerly and southeasterly morning glories were visible on the Bureau of Meteorology weather radar located at Mornington Island along with significant noise and clutter from the island and sea surface (figure not shown). Such lines are usually ascribed to echoes from insects (Doviak and Zrnić 1993), but in this case it is more likely that the echoes arise from the cloud particles themselves or from fluctuations in the

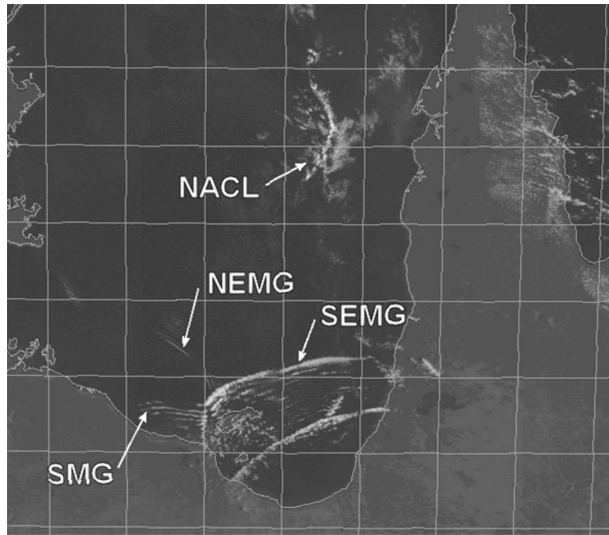


FIG. 6. Event 8: GMS satellite image of the gulf region at 0832 EST 9 Oct (2232 UTC 8 Oct). The four sets of cloud lines identified are the NACL, the southerly morning glory (SMG), the southeasterly morning glory (SEMG), and the northeasterly morning glory (NEMG).

radio refractive index of the air associated with the bores. Interestingly there was substantial sea clutter visible on the radar images at long range until the passage of the southeasterly line. As this line passed, the clutter behind it disappeared, indicating that a radio-propagation duct was being destroyed by the change in temperature and moisture structure accompanying the bore.

The radar data were used to produce an isochrone analysis of the lines (Fig. 8). While the radar cloud signatures were much reduced as they passed the island, they enable the phase speeds to be calculated. It was found that the southerly<sup>4</sup> line propagated at  $4 \text{ m s}^{-1}$  while the southeasterly line moved at  $16 \text{ m s}^{-1}$ . Nevertheless, time series taken at Sweers Island, shown in Fig. 7, suggest that the pressure amplitudes of southerly and southeasterly bores were comparable. The difference in speeds can be attributed at least in part to the fact that the waveguide seen by each disturbance is different because the component of the horizontal wind normal to each disturbance is different. The vertical wind profile ahead of the disturbances near Sweers Island is shown below (in Fig. 11 below).

<sup>4</sup> Actually, the radar shows an orientation near Mornington Island, which is slightly north of west to slightly south of east, but we continue to refer to it as the southerly disturbance on account of its broader scale orientation in the satellite imagery (see Fig. 6).

#### d. Aircraft observations

Segments of the aircraft track for event 8 are shown in Fig. 9. These include traverses at approximately constant altitude (segments 3, 5, and 6) and sloping ascents (segments 1, 4, and 7) or descents (segments 2 and 8) to or from a little over 3 km. Traverses 3 and 6 were made at approximately 255 m and traverse 5 at a little over 1100 m. The aircraft took off from Normanton Airfield at 0500 EST, about half an hour after the southeasterly disturbance had passed over the airfield. We restrict attention here to data from flight segments 1–5. The location of the waves as measured by the position of the crests and troughs in the vertical velocity field (see Figs. 12a and 15a below) during the traverses along tracks 3 and 5 are indicated by thin, straight lines (crests are solid lines, troughs are dashed) with the longer line segments referring to the measurements along traverse 3 and the shorter to traverse 5.

Figure 10 shows vertical profiles of virtual potential temperature,  $\theta_v$ , and mixing ratio,  $r$ , for the ascent behind the southeasterly morning glory, the descent ahead of it (segments 1 and 2 in Fig. 9, respectively), and the ascent near the axis of the inland trough (segment 4 in Fig. 9). The corresponding profiles of wind speed and direction are shown in Fig. 11. The  $\theta_v$  sounding ahead of the southeasterly morning glory (segment 2) is well mixed above 1 km with a strong stable layer below in which  $\theta_v$  increases by about 9 K from the surface. The two inland soundings (segments 1 and 4) are a little cooler below about 2.5 km. The two northernmost mixing ratio profiles show a sharp decrease with height in the lowest 300–400 m and the profile over the sea has a distinct minimum at 300 m. A similar minimum was recorded in the Karumba radiosonde sounding at 2230 EST 28 October (figure not shown) and is presumably a result of the advection of dry air from the land, probably associated with the return branch of the sea-breeze circulation (note that the corresponding wind profile shows a direction change from west to northwest below 250 m to east-southeast above that level). Shortly after passage of the southeasterly disturbance at Normanton, the wind was mainly southerly in the layer from 250 m to about 1.8 km.

Figure 12 shows time series of vertical velocity and the two horizontal wind components ( $U$  from the direction  $235^\circ$  and  $V$  from  $145^\circ$ ) during the traverse at a mean altitude of about 230 m through the southeasterly disturbance toward the southeast (track segment 3 in Fig. 9). The time series are plotted as functions of distance along the track. The direction of  $V$  is perpendicular to the leading cloud line as determined from the GMS satellite image at 0630 EST (not shown) and in

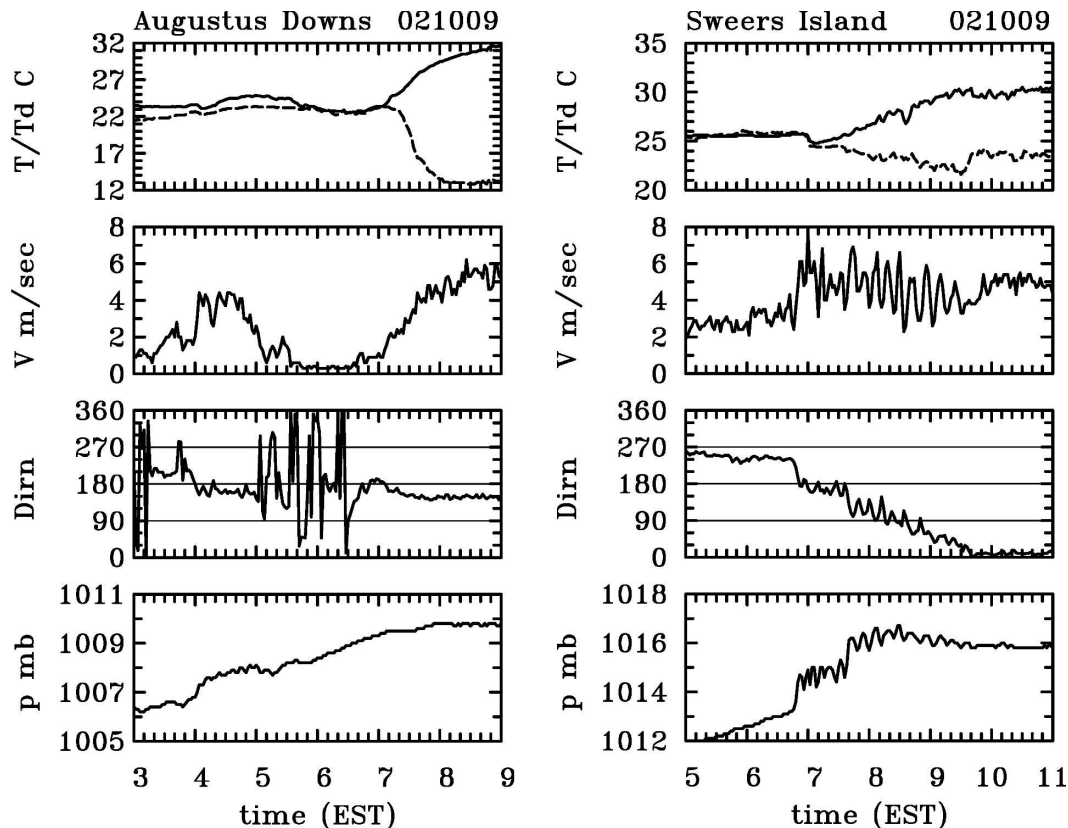


FIG. 7. Event 8: Time series of surface data at (left) Augustus Downs and (right) Sweers Island on 9 Oct 2002. Temperature ( $T$ , solid curve in top panels) and dewpoint temperature ( $T_d$ , dashed curve in top panels), wind speed ( $V$ ), direction (Dirn), and pressure ( $p$ ). The southerly morning glory arrived at Sweers Island at 0645 EST and the southeasterly arrived at 0740 EST.

the direction of motion of the cloud line, while  $U$  is parallel to the cloud line and to the right of its motion. The aircraft track is about  $12^\circ$  to the east of the line perpendicular to the cloud line except for a short segment near the leading waves (see Fig. 9). As the aircraft flew under the first cloud line, the wind changed abruptly from a westerly to a mean south-southwesterly, but with large amplitude oscillations in the cloud-normal component for about 40 km. Note that the wind speed component in the direction of propagation of the cloud lines is everywhere less than the propagation speed  $c$  ( $=16 \text{ m s}^{-1}$ ; see section 3c), consistent with the structure of a borelike disturbance. There are large oscillations also in the vertical velocity with an amplitude reaching  $3 \text{ m s}^{-1}$ . The average wavelength of the first four waves along the flight track is 5.6 km, calculated by projecting the distances between successive crests and troughs in the direction of the waves and averaging. When corrected for the Doppler shift associated with the wave speed and aircraft speed  $C$  ( $=78 \text{ m s}^{-1}$ ), the mean wavelength becomes  $5.6 \times (1 + c/C) = 6.7 \text{ km}$ .

Farther to the southeast, the winds were in the southwest sector until about 185 km, where they swung to east of south. Figure 13 shows the corresponding pressure trace and the radar height of the aircraft above the surface during this traverse. While the aircraft was set to fly at constant pressure, the presence of the waves led to large-amplitude excursions in the height ( $\pm 25 \text{ m}$ ). At this stage the aircraft was over the sea. The subsequent decline in height (bottom panel of Fig. 13) can be attributed in part to the increase in the height of the terrain along the flight track. Time series of temperature  $T$ , virtual potential temperature  $\theta_v$ , and water vapor mixing ratio  $r$  along this traverse are shown in Fig. 14. Note the abrupt decline in  $T$  and  $\theta_v$  and the sharp jump in  $r$  as the aircraft flew under the leading cloud line (at  $x = 15 \text{ km}$ ). These changes are evidence of the strong lifting that occurs at the leading edge of the bore wave, which, since  $\theta_v$  and  $r$  are conserved in clear air, would bring lower values of  $\theta_v$  and higher values of  $r$  to flight level (cf. the vertical profiles of  $\theta_v$  and  $r$  in the sounding ahead of the disturbance shown in Fig. 10). Both  $\theta_v$  and  $r$  relax back, more or less, to their original

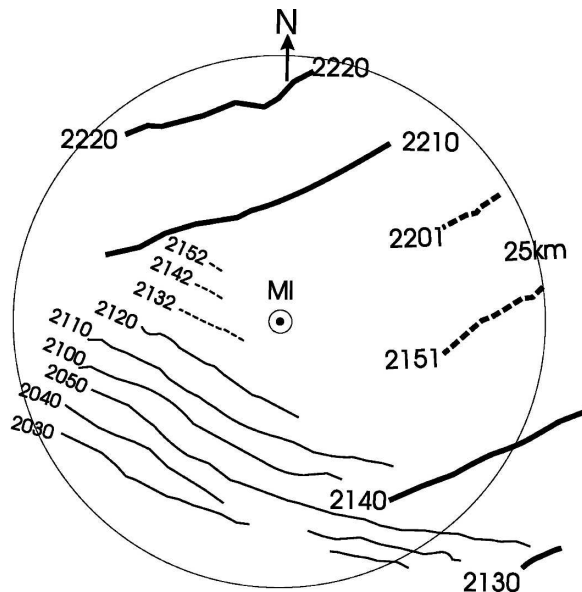


FIG. 8. Event 8: Isochrones of the southerly (thin lines) and southeasterly (thick lines) morning glories as they passed the Morningning Island radar (MI). The dashed lines indicate that the line was only visible at a radar tilt higher than the base scan. Each isochrone is labeled with the time in UTC. Also shown is the 25-km range ring from the radar.

values over a distance of 110–120 km from the leading edge of the bore.

Figure 15 shows time series of  $w$  and virtual potential temperature,  $\theta_v$ , during the traverse toward the west-northwest at a mean altitude of about 1100 m over the region of interaction between the southeasterly and southerly disturbances (track segment 5 in Fig. 9). The most striking feature of this figure is the large-amplitude vertical motions with peak upward and downward values reaching  $5 \text{ m s}^{-1}$ . Corresponding oscillations occurred also in the horizontal wind components where the mean motion is from the southeastern sector (figure not shown). A close comparison of the time series of  $w$  and  $\theta_v$  shows that these are a quarter of a wavelength out of phase, that is, the maximum and minimum values of  $\theta_v$  occur when  $w = 0$ . This is as it should be for stable internal gravity waves.

As far as we are aware, these are the first measurements of their type made with a well-instrumented research aircraft in and around a morning glory disturbance, although a few more rudimentary measurements were reported by Clarke et al. (1981).

#### 4. Other major events

Event 1 occurred at the beginning of the instrument deployment phase when only two AWS stations were in

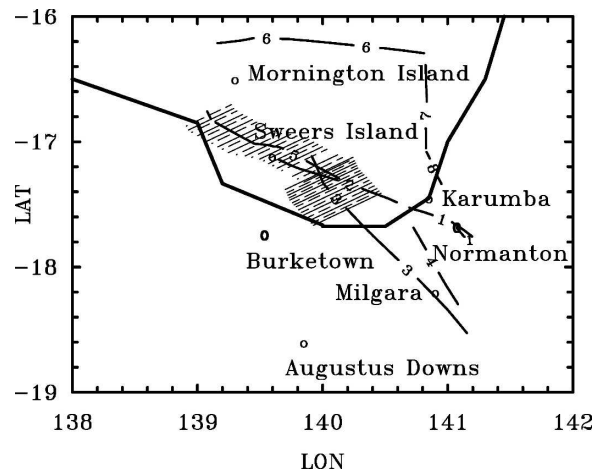


FIG. 9. Event 8: Aircraft soundings and traverses during the multiple disturbances of 9 Oct 2002. The sections of the flight are numbered sequentially: 1 = ascent from Normanton behind the southeasterly morning glory, primarily to the north-northwest, commencing at 0515 EST; 2 = descent ahead of the southeasterly morning glory, commencing at 0537 EST; 3 = traverse toward the south-southeast at an altitude of approximately 255 m (800 feet) through this disturbance, commencing at 0608 EST; 4 = ascent toward the north-northwest from the inland trough, commencing at 0701 EST; 5 = traverse at a mean altitude of approximately 1100 m over the region of interaction of the southeasterly and southerly morning glories, commencing at 0733 EST; 6 = traverse toward the east under the intersection of the three disturbances, commencing at 0819 EST; and 7 (8) = ascent (descent) over the eastern gulf, commencing at 0903 EST. The position of the crests and troughs in the vertical velocity field (see Figs. 11a, 14a) during the traverses along tracks 3 and 5 are indicated by thin, straight lines (troughs are dashed) with the longer line segments referring to the measurements along track 3.

operation. It is considered to be a major event because it was accompanied at Karumba by a spectacular series of cloud lines moving from the southwest (Fig. 16a) and a very clear cloud line in the visible satellite imagery (Fig. 16b). There were also clear borelike signatures in the surface pressure trace at Karumba commencing at 0645 EST and at Morningning Island at 0935 EST.

Figure 16c shows a visible satellite image for event 2 at 0830 EST 17 September. The southerly disturbance is clearly marked by four cloud lines stretching approximately west–east with the two northernmost lines over the southeastern part of the gulf. A northeasterly morning glory is marked by a series of north-northwest–south-southeast oriented cloud lines in the same region. The southerly disturbance was recorded at Augustus Downs at 0605 EST, Milgarra at 0730 EST, Burketown at 0745 EST, Karumba at 0820 EST, Sweers Island at 0850 EST, Morningning Island at 0945 EST, and Birri Beach at 1000 EST, but not at Vanrook, Dunbar, and Highbury on the peninsula. AWS data from

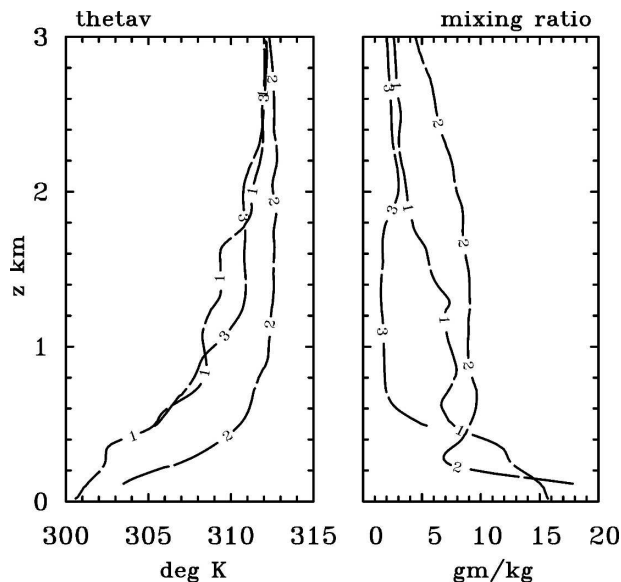


FIG. 10. Event 8: Vertical profiles of (left) virtual potential temperature  $\theta_v$ , and (right) mixing ratio  $r$ , for the ascent behind the southeasterly morning glory, the descent ahead of it (segments 1 and 2 in Fig. 9, respectively), and the ascent near the axis of the inland trough (segment 4 in Fig. 9).

Borrooloola, Delta Downs, and Croydon were not available on this day.

The satellite imagery during event 5 (see Fig. 2 in Part I) shows three disturbances: a northeasterly morning glory with many cloud lines in the southeast of the gulf, a gulf line to the northeast of it, and a southerly disturbance stretching several hundred kilometers to

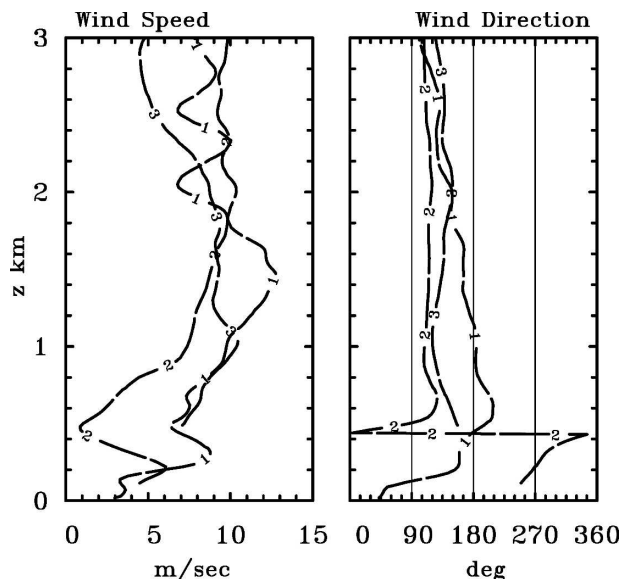


FIG. 11. As in Fig. 10 but for wind (left) speed and (right) direction.

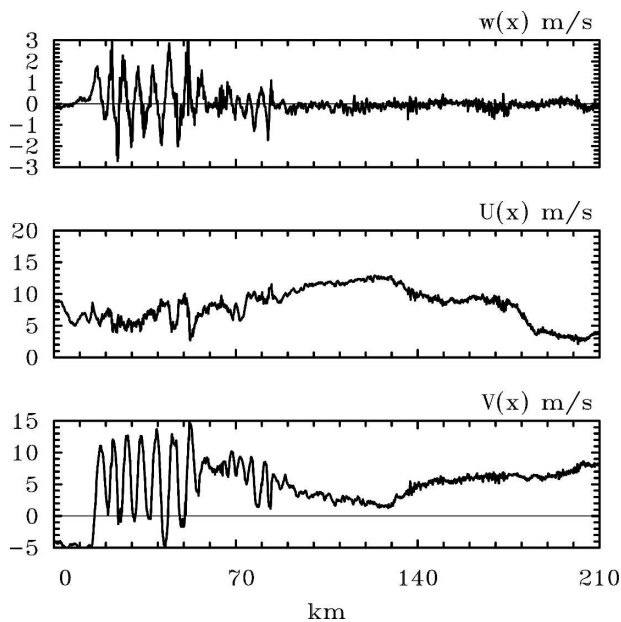


FIG. 12. Event 8: Time series of vertical velocity  $w$  and the two horizontal wind components ( $U$  from the direction  $235^\circ$  and  $V$  from  $145^\circ$ ) during the aircraft traverse at a mean altitude of about 230 m through the southeasterly disturbance toward the southeast (track segment 3 in Fig. 9). The time series are plotted with the abscissa measuring distance  $x$  along the track.

the west of the southernmost tip of the gulf. The disturbance produced clear signatures at stations west of Magowra, times of passage being 0420 EST at Augustus Downs, 0555 EST at Milgarra, 0530 EST at Burketown, 0800 EST at Mornington Island, 0655 EST at Sweers Island, and 0930 EST at Borrooloola. It was difficult to determine a time of passage at Birri Beach, where it arrived about the same time as the northeasterly morning glory.

On 14 October (event 9) both southerly and northeasterly morning glories were observed. The northeast-

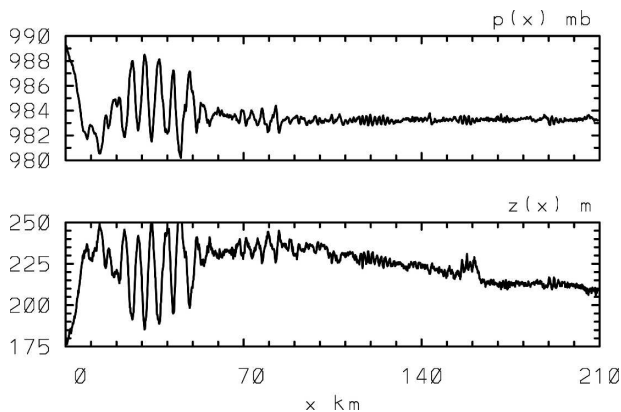


FIG. 13. As in Fig. 12 but for time series of pressure and radar height.

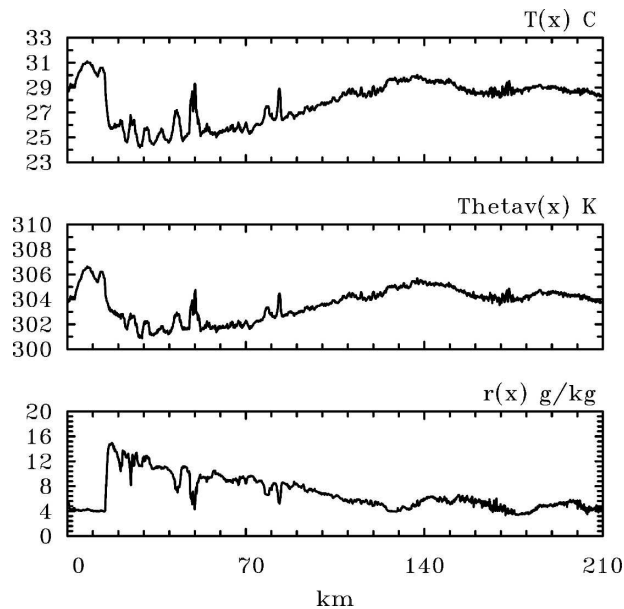


FIG. 14. As in Fig. 12 but for time series of temperature, virtual potential temperature, and water vapor mixing ratio.

erly was prominent in the satellite image at 0630 EST (not shown) and was recorded at all AWS stations. In contrast, the southerly disturbance did not seem to be associated with cloud, but it had a clear signature at most AWS stations, supporting its classification as a major event. Times of passage were 0300 EST at Borrooloola, 0325 EST at Augustus Downs, 0320 EST at Milgarra, 0530 EST at Burketown, 0725 EST at Mornington Island, 0730 EST at Birri Beach, 0435 EST at Magowra, 0445 EST at Karumba, 0600 EST at Delta Downs, and 0645 EST at Vanrook. Surprisingly, the signature at Sweers Island was not clear. The disturbance was not recorded at the two northernmost stations, Dunbar and Highbury. There was a clear dryline passage at Augustus Downs (about 1230 EST), Burketown (about 1110 EST), and Birri Beach (about 0930 EST), but not at other stations, including Mornington Island and Sweers Island (curiously because these two stations lie to the south of that at Birri Beach).

Composite MSLP analyses averaged for the six major events (events 1, 2, 4, 5, 8, and 9) (a) at 1600 EST on the day before the event and (b) at 0400 EST on the day of the event are shown in Figs. 17. Also shown are regions where the relative vorticity at 950 mb is less than  $-1 \times 10^{-5} \text{ s}^{-1}$  and  $-5 \times 10^{-5} \text{ s}^{-1}$ , respectively. As in events 4 and 8, the striking feature of the composite synoptic situation is the strong inland ridging that occurs over the northeastern part of the continent with a trough line oriented approximately along or parallel to the southern coastline of the gulf on the day of passage. The marked strengthening of the inland trough during the

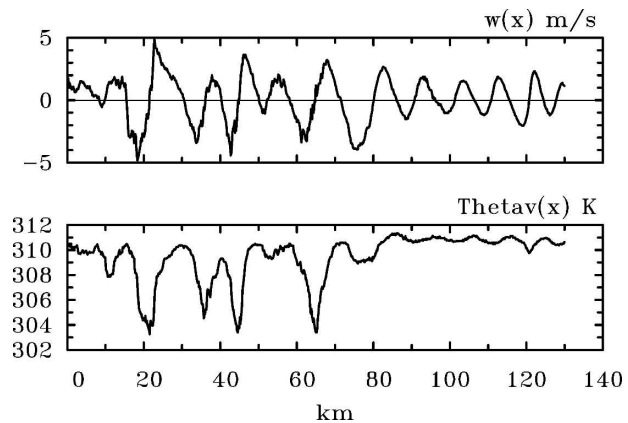


FIG. 15. Event 8: Time series of vertical velocity  $w$  and virtual potential temperature during the traverse at a mean altitude of a little over 1100 m over the southeasterly disturbance toward the west-northwest (track segment 5 in Fig. 9). The time series are plotted with the abscissa measuring distance  $x$  along the track, which is nearly opposite to the direction in Figs. 12–14 and a little to the left of the direction of motion of the disturbance (see Fig. 9).

night is clearly evident in the strip of high relative vorticity south of the gulf at 0400 EST. On the day prior to events 2, 4, 5, and 9 there was a pronounced ridge along the east coast of Australia, which is conducive to the formation of northeasterly morning glories. This ridge is also apparent in the composite fields.

## 5. Discussion

While the classification of events as major or minor is based partly on subjective judgment, the synoptic situation for the latter is markedly different from the former. This is seen in Figs. 17c,d, which show composite MSLP and 950-mb vorticity analyses similar to those in Figs. 17a,b, but averaged for the five minor events (events 3, 6, 7, 10, and 11). These composites are broadly representative of the individual days. Note that the center of the midlatitude anticyclone lies farther to the east than in Figs. 17a,b and the ridge is almost meridional. Furthermore, in contrast to major events, one does not see strong ridging to the south during the preceding 12 h. A strip of enhanced negative vorticity still lies south of the gulf at 0400 EST, but the magnitude is much weaker than for the major events. The ridge along the coast is still a prominent feature and there is a strip of strong vorticity near the western side of Cape York Peninsula at 0400 EST, indicative of the convergence line associated with northeasterly morning glories. At this stage the factors that distinguish the generation of minor events from that of major events are poorly understood and are the subject of continuing investigation.

With the experience gained during previous studies

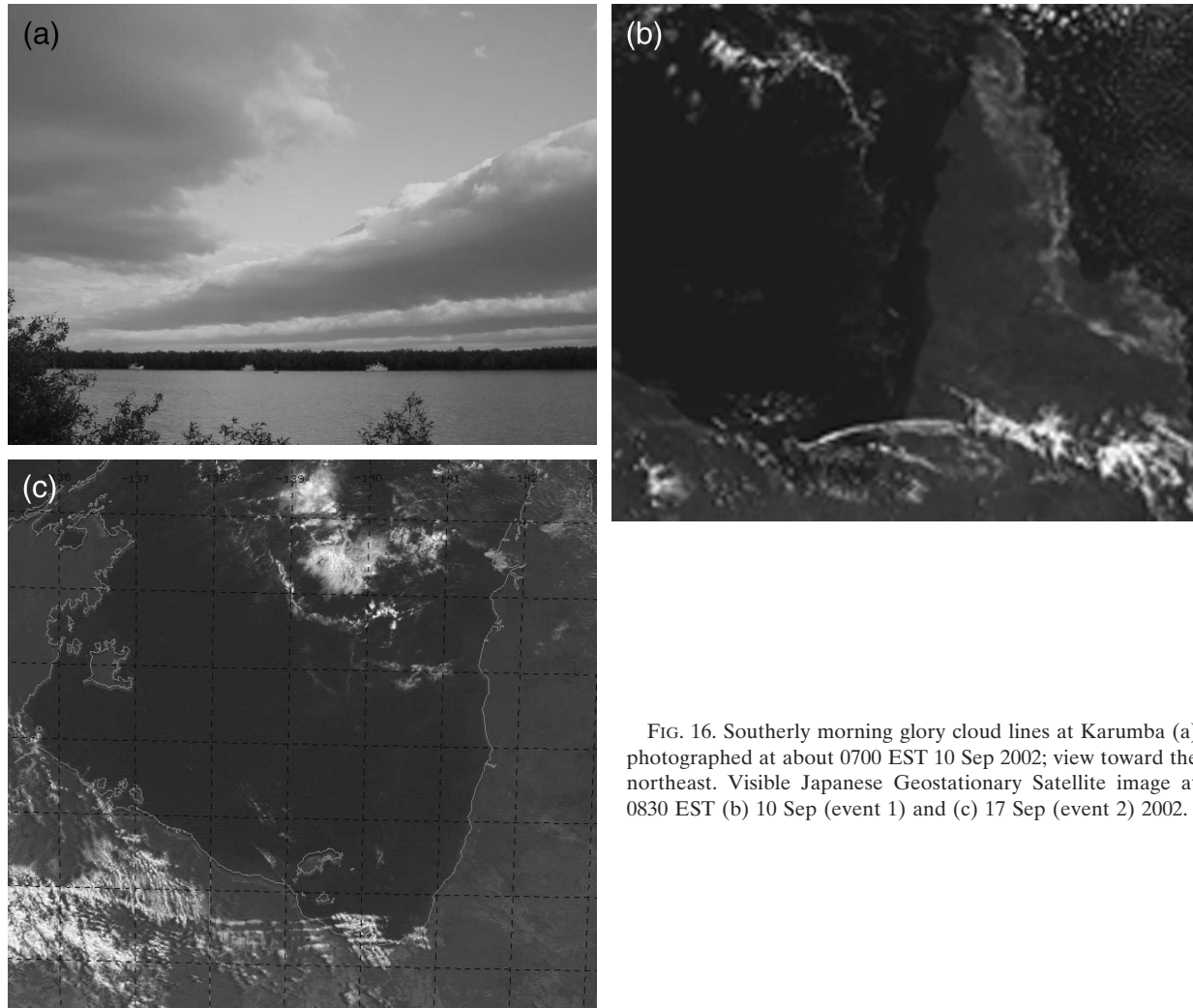


FIG. 16. Southerly morning glory cloud lines at Karumba (a) photographed at about 0700 EST 10 Sep 2002; view toward the northeast. Visible Japanese Geostationary Satellite image at 0830 EST (b) 10 Sep (event 1) and (c) 17 Sep (event 2) 2002.

of southerly morning glories (Smith et al. 1982, 1986) and early on in the GLEX experiment itself, we were able to anticipate event 8 one week ahead on the basis of the extended range forecast of mean sea level pressure by the Bureau of Meteorology's Global Analysis and Prediction System. This ability was fortunate and contributed greatly to the success of the aircraft mission described in section 3d.

The analyses of sections 3 and 4 showed that the major southerly disturbances occurred overnight when there was strong ridging over the continent to the south on the previous day and the inland trough lay just south of the gulf the following night. This result is brought out in Fig. 18, which is a time series of surface pressure at Augustus Downs at 2200 EST each evening during 43 days of measurement there. The days with southerly disturbances are highlighted by solid vertical lines. Peaks in the pressure trace reflect the passage or strengthening of the ridge to the south. Note that the

events on the mornings of 17, 23, and 29 September and 9 and 14 October occurred on days where the pressure at 2200 EST that evening had increased during the previous 24 h. The increase was particularly large for the two major events of 28–29 September and 9 October. However, the events of 4, 5, 6, 20, and 21 October, which were mostly weak disturbances, occurred during periods when the 2200 EST pressure fell during the previous 24-h period, suggesting that strong ridging to the south is not a prerequisite for triggering disturbances. Indeed, an inspection of individual MSLP charts indicates that weaker disturbances occurred when the ridge to the south was quasi-stationary, as suggested by the composite plots for minor events shown in Fig. 18. It is interesting to note the tendency for minor events to occur on consecutive days (events 6 and 7, events 10 and 11) and that events 6 and 7 followed on the days after major event 5.

It has been noted previously that synoptic conditions

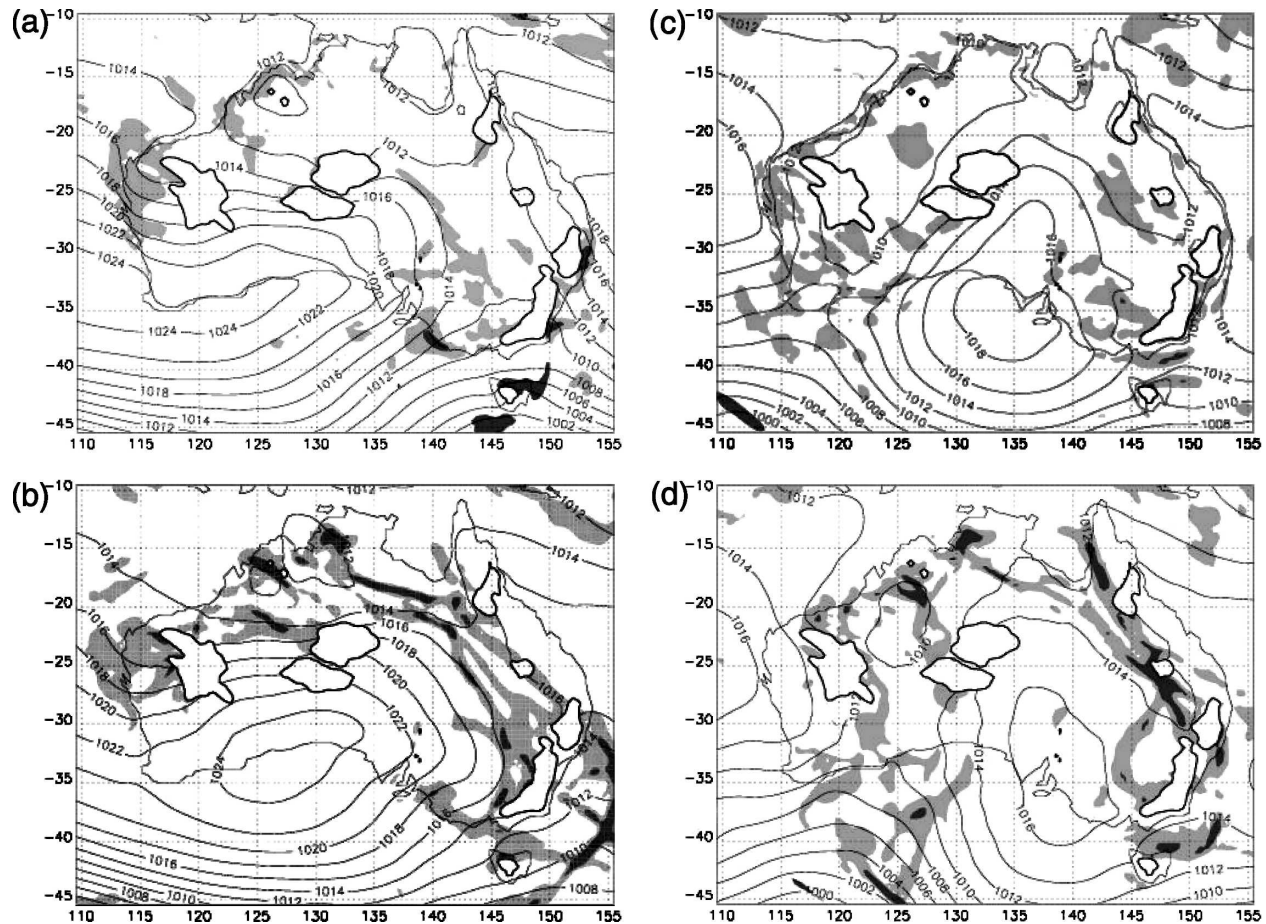


FIG. 17. Composite MSLP analyses averaged for the six major events (events 1, 2, 4, 5, 8, and 9) at (a) 1600 EST on the day before the event and (b) 0400 EST on the day of the event; (c), (d) similar composites for the five minor events (events 3, 6, 7, 10, and 11). The light and dark shaded regions in each panel show where the relative vorticity at 950 mb is less than  $-1 \times 10^{-5} \text{ s}^{-1}$  and  $-5 \times 10^{-5} \text{ s}^{-1}$ , respectively.

conducive for the generation of southerly disturbances tend to coincide with those favorable for the generation of northeasterly disturbances (morning glories or NA-CLs; see, e.g., Smith et al. 1986). In at least 5 of the 11 southerly events detailed above (events 2, 5, 8, 9, and 10), northeasterly disturbances were recorded also. The meso-LAPS predictions during GLEX also showed the formation of a northeasterly disturbance almost daily, and on most occasions the model succeeded in predicting a southerly disturbance when one was observed. The performance of meso-LAPS during the experiment will be examined in Weinzierl et al. (2006, manuscript submitted to *Wea. Forecasting*).

All borelike disturbances were fully formed when they reached the southernmost stations in the network. Observations of the genesis stages of the bores were not obtained, but the numerical model simulations of the events do shed light on this question. For example, the high-resolution (3-km horizontal grid) simulation by Thomsen and Smith (2006) of event 4 shows that the

bore emerged from the collision of the northward-moving front following its collision with the sea-breeze front from the southern gulf coast.

Observations taken of the morning glory show that the waves are of large amplitude, yet the extent to which linear theory is relevant is still uncertain. On one hand, linear theory has been invoked with success to explain, at least qualitatively, why the waves generated in simple numerical models are able to propagate over large horizontal distances with little attenuation (see, e.g., Crook 1986, 1988). On the other hand, Menhoffer et al. (1997) have shown that, to the extent that linear theory is applicable, the observed duct in which the morning glory propagates is highly imperfect and allows wave energy to radiate vertically. For this reason they conclude that the waves must be continuously forced. This idea was reinforced by the numerical simulations of Smith and Noonan (1998) and Goler and Reeder (2004). In particular, the latter authors show how waves at the leading edge of the bore are continuously

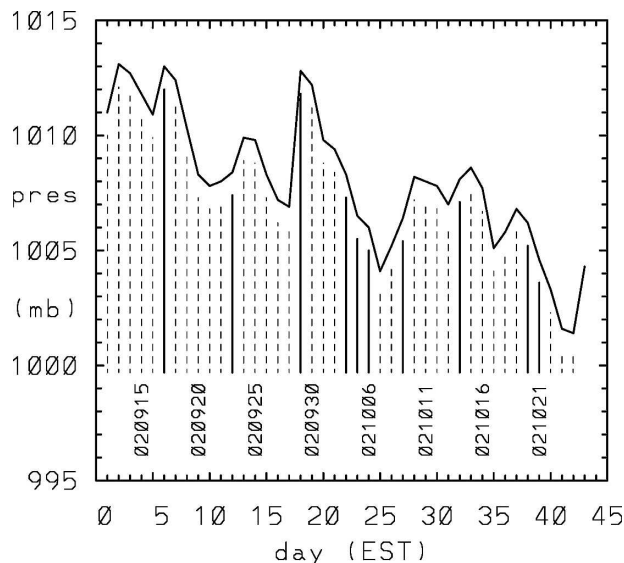


FIG. 18. Time series of surface pressure at Augustus Downs at 2200 EST (solid line) each evening during 43 days of measurement there. The days with southerly disturbances are highlighted by solid vertical lines and other days by dashed lines.

generated as it propagates offshore and over the gulf.

According to linear theory the vertical wavenumber  $m$  is related to the environmental conditions through the relation  $m^2 = N^2/(V - c)^2 - V_{zz}/(V - c) - k^2 = l^2(z) - k^2$ , where  $k$  is the horizontal wavenumber,  $N(z)$  is the Brunt-Väisälä frequency,  $V(z)$  is the background wind speed in the direction of wave propagation,  $c$  is the phase speed of the waves, and  $l(z)$  is the Scorer parameter. Small-amplitude waves propagate vertically when  $m$  is real but are evanescent when  $m$  is imaginary. Consequently, linear theory predicts that waves may be ducted when the environmental conditions allow propagation in a restricted layer only. One such configuration, thought to be important for trapped low-level disturbances such as the morning glory, is a stable surface-based layer permitting vertical propagation beneath a deep layer in which the Scorer parameter is sufficiently small to suppress the upward propagation of the waves. Three relevant situations in which the Scorer parameter decreases with height are when the Brunt-Väisälä frequency decreases with height, when the background wind speed increases with height, or when the curvature changes sign from negative in the stable surface layer to positive aloft.

Figure 19 shows vertical profiles of the square of the Scorer parameter  $l^2$  and the contribution of the buoyancy term  $N^2/(V - c)^2$  to it. The difference between these curves is simply the contribution from the curvature term,  $V_{zz}/(V - c)$ . As in section 3d,  $V$  is the component in the direction of the waves,  $c = 16 \text{ m s}^{-1}$ , and  $V - c < 0$  at all heights. The profiles plotted have been

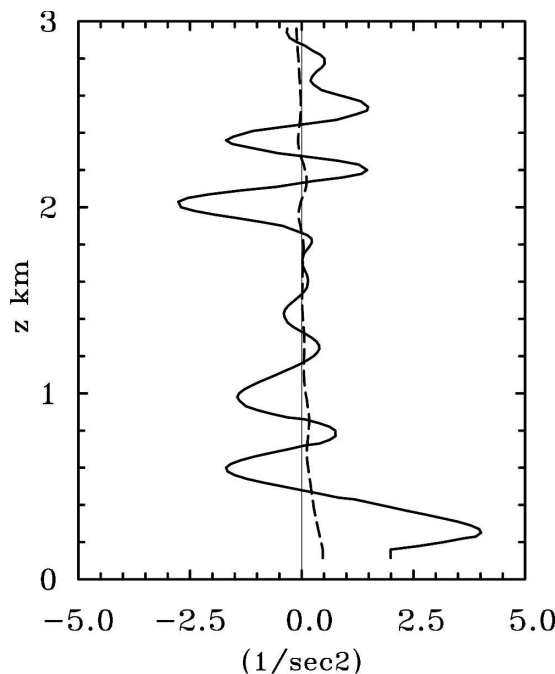


FIG. 19. Event 8: Vertical profiles of the Scorer parameter squared  $l^2$  (solid curve) and the contribution to it from the term  $N^2/(V - c)^2$  (dashed curve). Units in  $10^{-3} \text{ s}^{-2}$ .

smoothed greatly as  $V_{zz}$  is very noisy. While the environment in which the southeasterly morning glory propagates comprises a deep nearly neutral layer above a stably stratified surface layer (Fig. 9),  $l^2(z)$  is dominated by the curvature term, even in the surface-based stable layer. While the curvature term is mostly positive in approximately the lowest 250 m, it is not uniformly negative above. For these reasons, the longevity of the morning glory does not appear to be explained by the vertical structure of the Scorer parameter.

### 6. Conclusions

The much longer time series of surface data acquired during GLEX compared with previous experiments highlights the regularity of the occurrence of convergence lines propagating from the south in the southern gulf region. Favorable synoptic conditions for the generation of these lines were found to be similar to those in earlier studies. Major disturbances tend to be accompanied by strong ridging from the south on the previous day, but weaker disturbances may occur when the ridge is quasi stationary or even slightly retreating. Conditions conducive to the generation of southerly convergence lines often coincide with those favorable for northeasterly lines so that southerly morning glories frequently occur on the same day as northeasterly morning glories, depending on the strength and timing of the southerly disturbance.

Highlights of the present experiment were the documentation of a borelike disturbance moving ahead of an airmass change in the form of a dryline and a unique set of detailed aircraft observations that were obtained through and around a series of three morning glory disturbances. The aircraft data for the southeasterly disturbance show coherent waves near the leading edge of the disturbance with a wavelength of about 6 km. Measured vertical velocities were as high as  $3 \text{ m s}^{-1}$  on a traverse at 800 m and even higher aloft ( $5 \text{ m s}^{-1}$  at an altitude of 1 km), where waves from two disturbances were interacting. There were large oscillations also in the wind component in the direction of propagation of the disturbance but not in the component parallel to the disturbance. Moreover, the wind speed component in the direction of propagation was everywhere less than the propagation speed. Thus, the data support the borelike nature of the disturbance.

Although the environment in which the southeasterly morning glory propagates comprises a deep nearly neutral layer above a stably stratified surface layer, the stability term in the Scorer parameter is much smaller than the curvature term, even in the surface-based stable layer. While the latter term is mostly positive in approximately the lowest 250 m, suggesting that the low-level jet observed over the gulf augments the waveguide on which the morning glory propagates, the term is not uniformly negative above. Thus, the longevity of the morning glory does not appear to be explained by the nonleakiness of the waveguide.

The cloud lines were visible on radar, suggesting that the radar echoes arise from the cloud particles or from fluctuations in the radio refractivity index of the air in the waves. Substantial sea clutter observed in the radar images at long range before the passage of the southeasterly disturbance of event 8 disappeared after the passage, indicating that a radio-propagation duct was destroyed by the change in temperature and moisture structure accompanying the bore.

*Acknowledgments.* We thank the Australian Bureau of Meteorology for its support, especially the Queensland and Northern Territory Regional Offices and the Bureau of Meteorology Research Centre. We are grateful to the following participants from Monash University, University of British Columbia, Airborne Research Australia, and the University of Munich: Andrew Coutts, Rudi Gaissmaier, Thomas Hamburger, Jorg Hacker, Gabriel Kalotay, Carsten Kykal, Heinz Lösslein, Andreas Ropuack, Thomas Spengler, Brian Seymour, Bernadett Weinzierl, Hilbert Wendt, and

Hongyan Zhu. We also thank Sarah Arnup (Monash University) for her help with Figs. 21 and 25. Funding for the experiment came from the Australian Bureau of Meteorology, the German Research Council (Deutsche Forschungsgemeinschaft), and Monash University.

#### REFERENCES

- Clarke, R. H., R. K. Smith, and D. G. Reid, 1981: The morning glory of the Gulf of Carpentaria: An atmospheric undular bore. *Mon. Wea. Rev.*, **109**, 1726–1750.
- Crook, N. A., 1986: The effect of ambient stratification and moisture on the motion of atmospheric undular bores. *J. Atmos. Sci.*, **43**, 171–181.
- , 1988: Trapping of low-level internal gravity waves. *J. Atmos. Sci.*, **45**, 1533–1541.
- Deslandes, R., M. J. Reeder, and G. Mills, 1999: Synoptic analyses of a subtropical cold front observed during the 1991 Central Australian Fronts Experiment. *Aust. Meteor. Mag.*, **48**, 87–110.
- Doviak, R. J., and D. S. Zrnić, 1993: *Doppler Radar and Weather Observations*. Academic Press, 562 pp.
- Goler, R. A., and M. J. Reeder, 2004: The generation of the morning glory. *J. Atmos. Sci.*, **61**, 1360–1376.
- , —, R. K. Smith, H. Richter, S. Arnup, T. Keenan, P. May, and J. Hacker, 2006: Low-level convergence lines over northeastern Australia. Part I: The North Australian cloud line. *Mon. Wea. Rev.*, **134**, 3092–3108.
- Jackson, G. E., R. K. Smith, and T. Spengler, 2002: The prediction of low-level mesoscale convergence lines over northeastern Australia. *Aust. Meteor. Mag.*, **51**, 13–24.
- Menhofer, A., R. K. Smith, M. J. Reeder, and D. R. Christie, 1997: Morning Glory disturbances and the environment in which they propagate. *J. Atmos. Sci.*, **54**, 1712–1725.
- Preissler, M., M. J. Reeder, and R. K. Smith, 2002: A case study of a heat low over central Australia. *Aust. Meteor. Mag.*, **51**, 155–163.
- Puri, K., G. S. Dietachmayer, G. A. Mills, N. E. Davidson, R. A. Bowen, and L. W. Logan, 1998: The new BMRC Limited Area Prediction system, LAPS. *Aust. Meteor. Mag.*, **47**, 203–223.
- Reeder, M. J., D. R. Christie, R. K. Smith, and R. Grimshaw, 1995: Interacting morning glories over northern Australia. *Bull. Amer. Meteor. Soc.*, **76**, 1165–1171.
- , R. K. Smith, R. Deslandes, N. J. Tapper, and G. A. Mills, 2000: Subtropical fronts observed during the 1996 Central Australian Fronts Experiment. *Aust. Meteor. Mag.*, **49**, 181–200.
- Smith, R. K., and R. N. Ridley, 1990: Subtropical continental cold fronts. *Aust. Meteor. Mag.*, **38**, 191–200.
- , and J. A. Noonan, 1998: On the generation of low-level mesoscale convergence lines over northeastern Australia. *Mon. Wea. Rev.*, **126**, 167–185.
- , N. A. Crook, and G. Roff, 1982: Morning Glory: An extraordinary atmospheric undular bore. *Quart. J. Roy. Meteor. Soc.*, **108**, 937–956.
- , M. J. Coughlan, and J. Evans-Lopez, 1986: Southerly nocturnal wind surges and bores in northeastern Australia. *Mon. Wea. Rev.*, **114**, 1501–1518.
- , M. J. Reeder, N. J. Tapper, and D. R. Christie, 1995: Central Australian cold fronts. *Mon. Wea. Rev.*, **123**, 19–38.
- Thomsen, G., and R. K. Smith, 2006: Simulations of low-level convergence lines over northeastern Australia. *Quart. J. Roy. Meteor. Soc.*, **132**, 691–707.